Supplementary Information

Supplementary figures

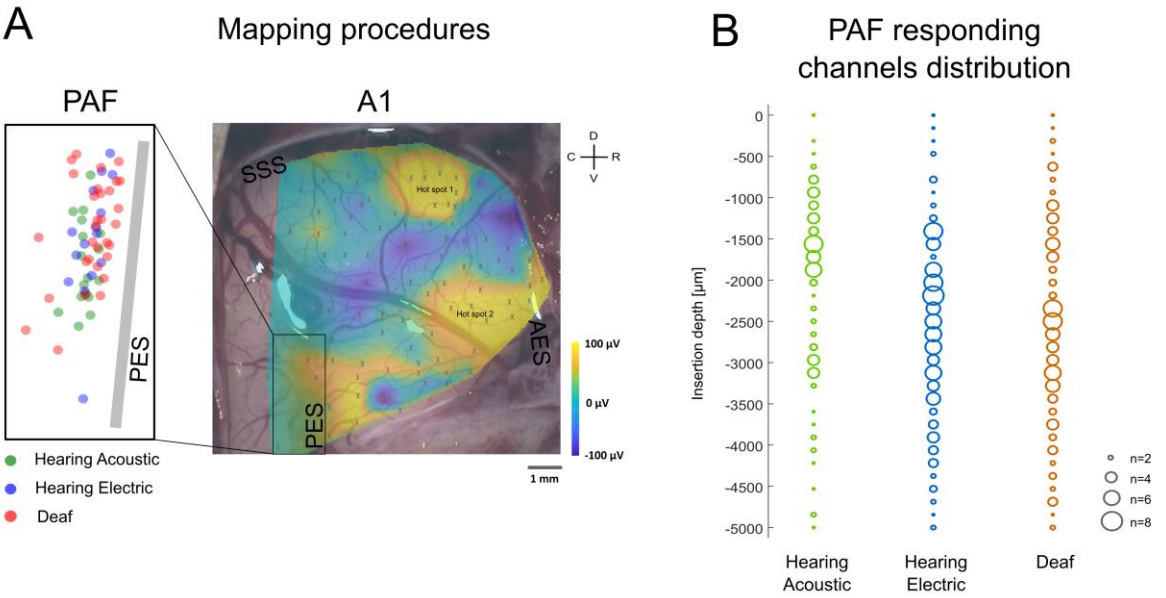

Supplementary Figure 1. Schematic illustration of the functional mapping in PAF and A1.

(A) Recording positions in A1 were determined by cortical surface LFP mapping and subsequent penetrations were in the hot spots (comp. Kral et al., 2009), whereas in PAF this was not possible due to its location within the PES. For this reason, penetrations in PAF mapped the whole extend of the field (inset on the left). A1 mapping is shown by an overlay of a photograph from one individual animal and the amplitudes of the P_a/N_b complex of the LFP (shown color coded). Crosses correspond to exact location of the recordings for construction of the activation map. **(B)** Distribution of PAF unit responses for all animals pooled based on penetration depth. The number of responding sites is proportional to the circle radius. Best responsive sites were in the middle of the penetration. A1 = primary auditory cortex, PAF = posterior auditory field, PES = posterior ectosylvian sulcus, SSS = suprasylvian sulcus, AES = anterior ectosylvian sulcus, V=ventral, D=dorsal, R=rostral, C=caudal.

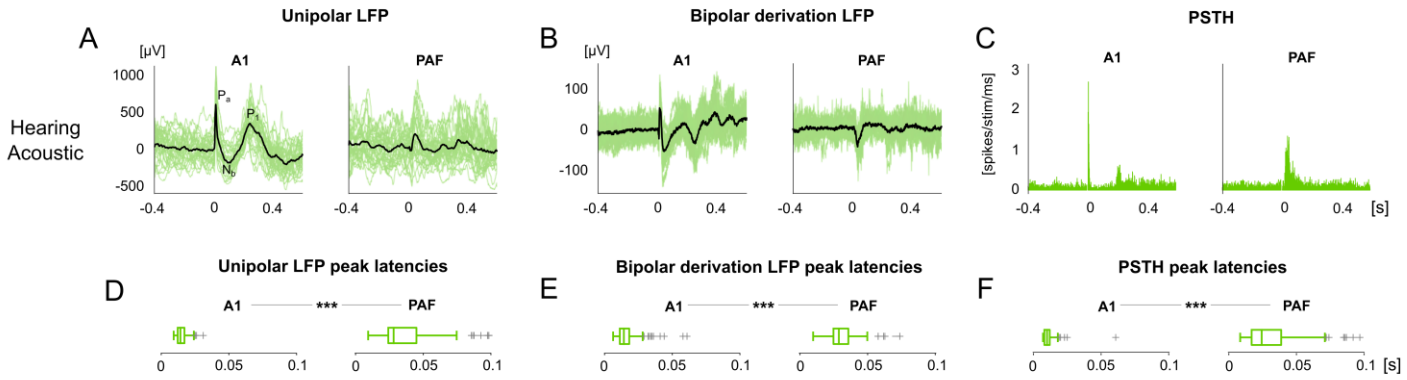

Supplementary Figure 2. LFP and unit responses in an acoustically-stimulated hearing control.

(A) Unipolar LFP examples in field A1 and PAF in an acoustically-stimulated hearing control. Individual trials and their average are shown in color and black, respectively. **(B)** Same as A for b-LFP responses. **(C)** Same as A for multiunit responses. **(D)** The peak-latencies for unipolar LFPs were in A1: 14.96 ± 3.90 ms, in PAF: 35.70 ± 18.09 ms (mean±SD). **(E)** Same as D for b-LFPs (A1: 15.62 ± 6.91 ms, PAF: 31.09 ± 10.30 ms). **(F)** Same as D for multi-unit activity peak-latencies (A1: 9.83 ± 3.04 ms, PAF: 24.50 ± 11.20 ms). All responses were evoked by acoustic click at intensity of 40 dB (acoustic) above site-threshold (see Method). D-F show significantly longer peak latencies in PAF than in A1 ($p<0.001$, two-tailed Wilcoxon rank-sum test).

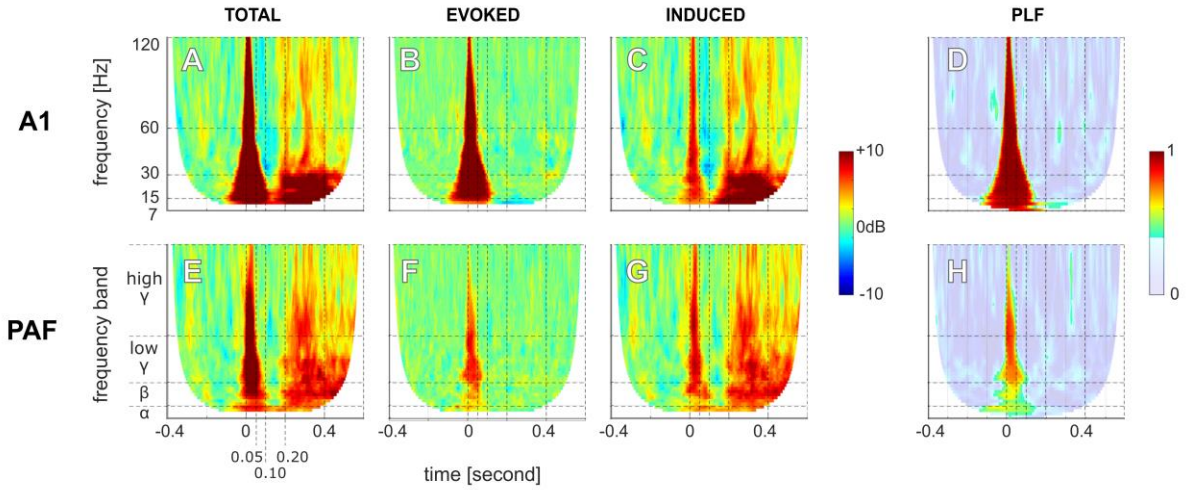

Supplementary Figure 3. TFR of the responses in an acoustically-stimulated hearing control.

TFRs of total (left panel, A, E), evoked (middle, B, F), induced (right, C, G) responses, and phase-locking factor (far right, D, H) in the primary A1 (upper panel, A-D) and the higher order PAF (lower panel, E-H) from an acoustically-stimulated hearing control, obtained from b-LFP signals. Data in (A-C,E-G) are shown in decibel relative to baseline (-400 ms to -100 ms pre-stimulus). Data in (D, H) are masked with critical value $p<0.01$. All responses were evoked by acoustic click at intensity of 40 dB (acoustic) above site-threshold (see Method). PLF = phase-locking factor.

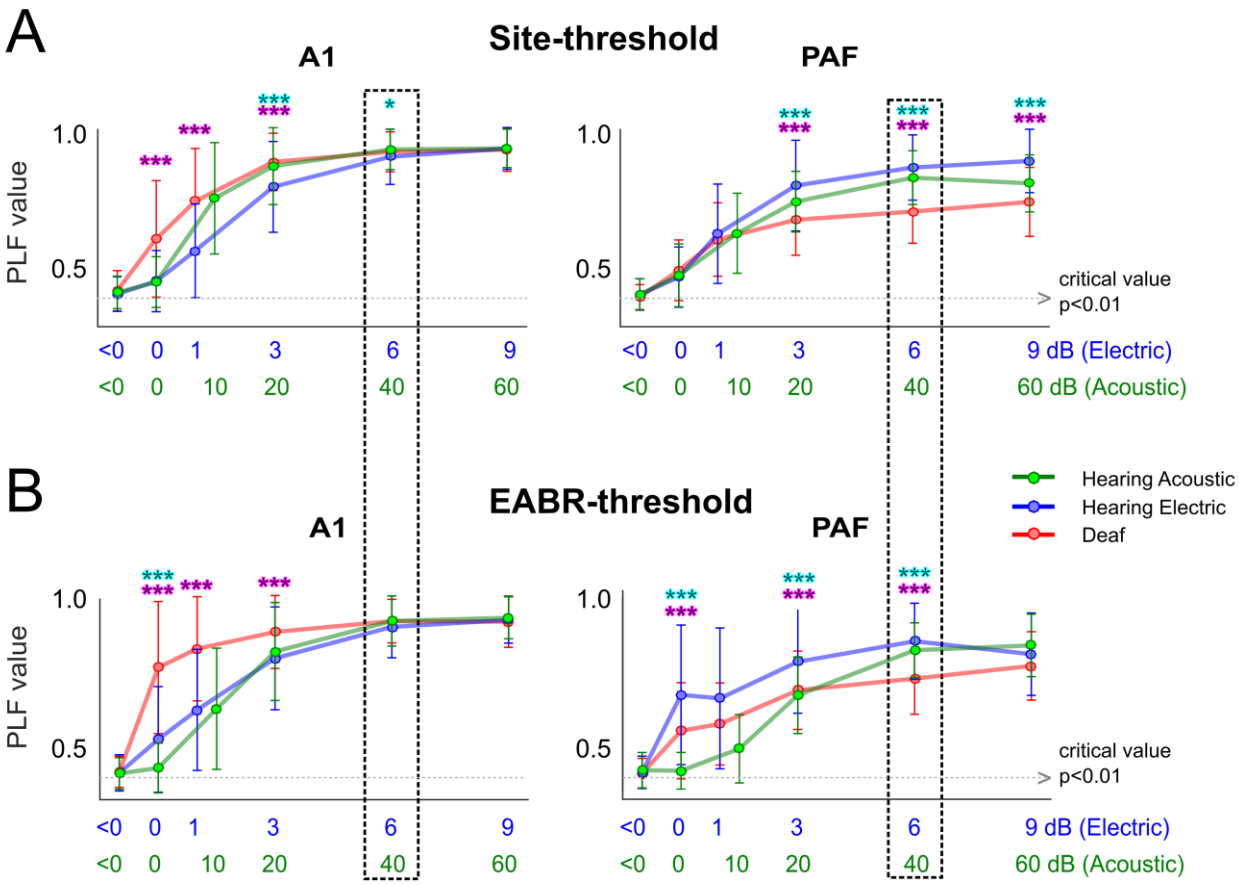

Supplementary Figure 4. Level functions.

(A) Level functions of the maximum early-response PLF-value computed relative to site-threshold. Acoustically-stimulated hearing controls are shown in green, electrically-stimulated in blue, and congenitally deaf in red in field A1 and PAF. **(B)** Same as A computed relative to acoustic and electric ABR-threshold. Statistical comparisons were performed using two-tailed Wilcoxon rank-sum test (with Bonferroni correction) for comparing acoustically- vs. electrically-stimulated hearing controls (cyan asterisks) and electrically-stimulated hearing vs. deaf animals (magenta asterisks). For further comparisons, the stimulation at 40 dB (acoustic) and 6 dB (electric) above threshold were used. At these levels, differences between hearing and deaf animals in the field A1 disappeared and the functions reached saturation. The critical value (dotted lines) represents the statistical threshold for PLF (see Materials and Methods). * ~ p<0.05; *** ~ p<0.001.

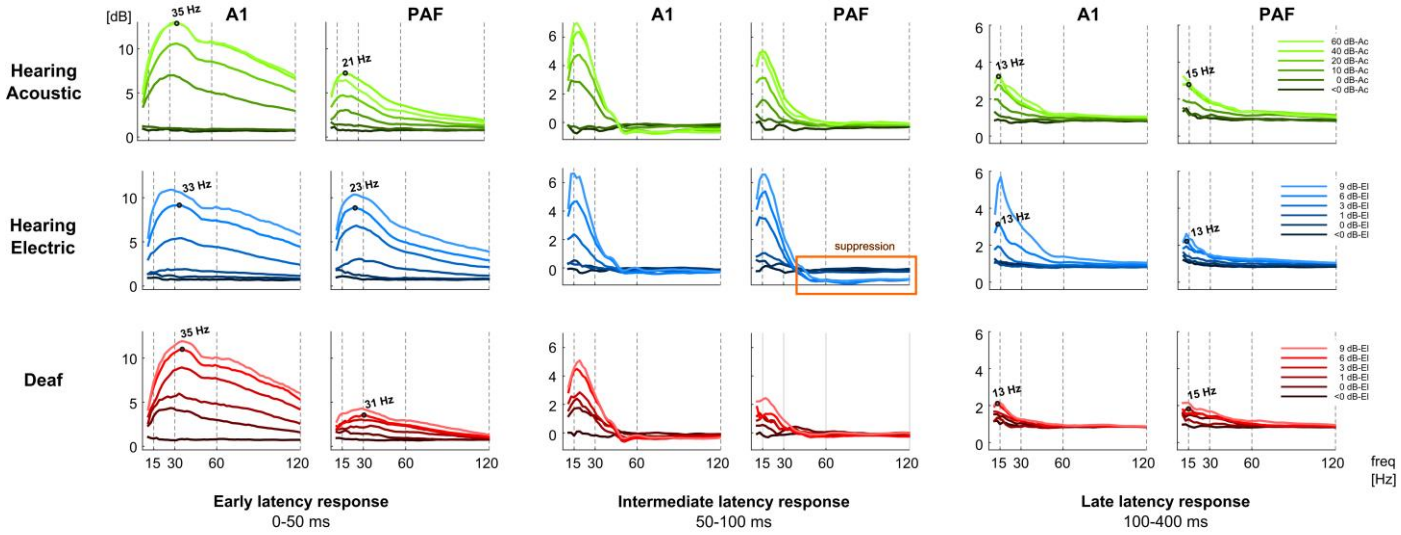

Supplementary Figure 5. Spectral responses at different stimulus intensities.

Grand mean of the spectra in A1 and PAF of acoustically-stimulated hearing controls (dark to light green lines) at intensities <0, 0, 10, 20, 40, 60 dB (acoustic), for electrically-stimulated hearing controls (dark to light blue lines) and for congenitally deaf cats (dark to light red lines), both at levels <0, 0, 1, 3, 6, 9 dB (electric). All levels are relative to the site-threshold (denoted as 0 dB). The spectra were computed by collapsing the time window of the baseline-corrected TFR results in early-latency (0-50 ms), intermediate-latency (50-100 ms), and late-latency (100-400 ms) post-stimulus. Only positive TFR values were included in the early-latency and late-latency response to capture solely the activations. All data are shown in dB baseline. Numbers in Hz show spectral maxima, each for 40 dB (acoustic) and 6 dB (electric) above threshold.

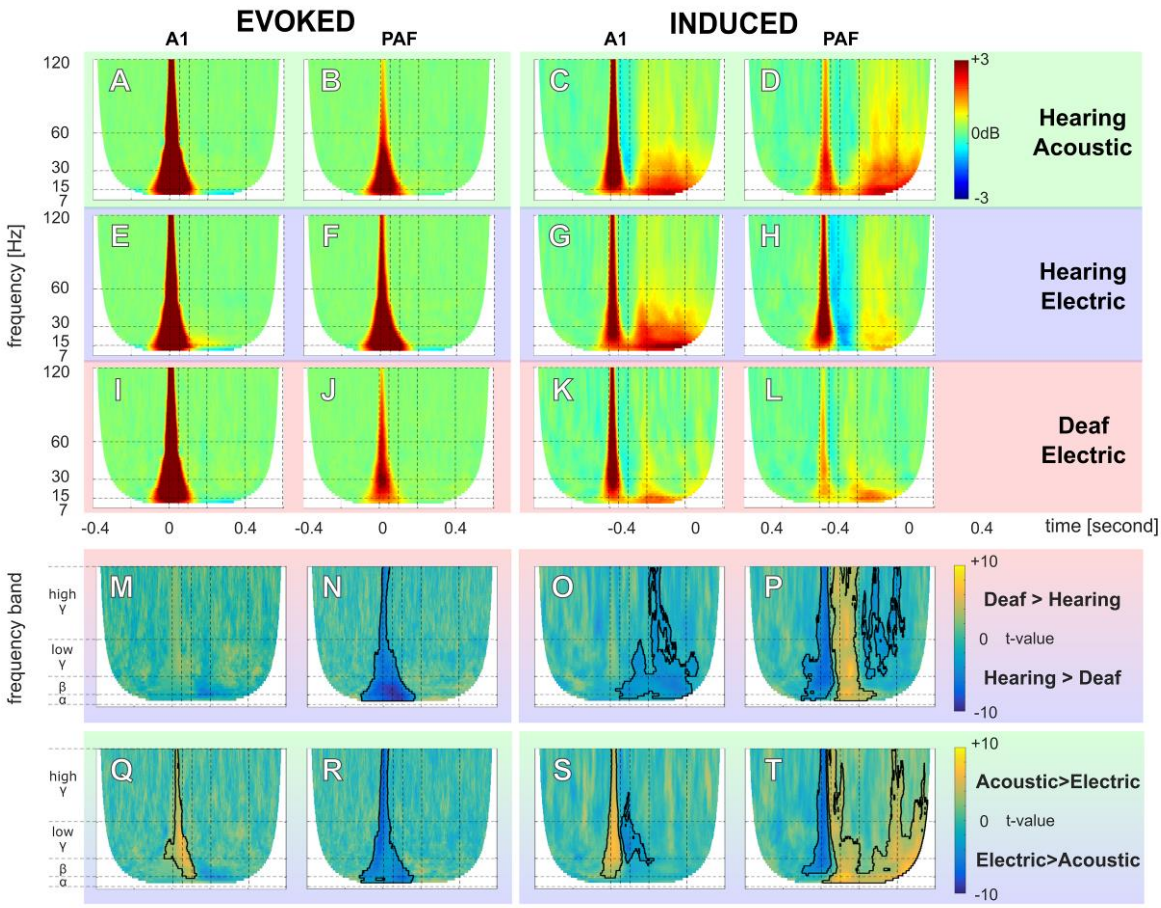

Supplementary Figure 6. Grand mean and statistical comparison of evoked and induced TFR with acoustic and electric ABR-threshold.

(A-L) Grand mean of evoked (A,B,E,F,I,J) and induced (C,D,G,H,K,L) TFR responses from b-LFP in acoustically-stimulated hearing controls (green background, A-D), electrically-stimulated hearing controls (blue background, E-F), and congenitally deaf cats (red background, I-L) in field A1 and PAF. All TFRs are shown in decibel relative to baseline (-400 ms to -100 ms pre-stimulus). Here, responses at 40 dB (acoustic) above ABR-threshold and 6 dB (electric) above E-ABR-threshold were compared. **(M-T)** Non-parametric cluster-based permutation statistical testing (cluster α threshold 1%, two-tail significant α value=0.5%) for hearing vs. deaf comparison (M-P) and acoustic vs. electric comparison (Q-T). Data are shown in t-values, significant regions are outlined by black lines. **(M)** Evoked response comparison in A1 (panel E and I). **(N)** Evoked response comparison in PAF (panel F and J). **(O)** Induced response comparison in A1 (panel G and K). **(P)** Induced response comparison in PAF (panel H and L). **(Q)** Evoked response comparison in A1 (panel A and E). **(R)** Evoked response comparison in PAF (panel B and F). **(S)** Induced response comparison in A1 (panel C and G). **(T)** Induced response comparison in PAF (panel D and H).

Supplementary materials and methods

Cochlear implant (CI)

The CI consisted of a medical-grade silicone tube with five intrascalar contacts: A small golden sphere at the tip (diameter 0.8mm) and four golden rings, with a distance of 1 mm between all electrodes (Behrendt, 1999). The intrascalar part of the implant was tapered in the apical direction from a diameter of 1.6–0.8 mm. The gold contacts were connected to a seven-strand Teflon-coated stainless-steel braided wire. The extracochlear silicone tube had a diameter of 1.6 mm. The stimulation mode was wide bipolar (most apical vs. the fourth intracochlear electrode in the basal direction; the distance between active electrodes was thus 3 mm).

To ensure that insertion depth was comparable, the electrode array was inserted until the most basal electrode of the implant was just observed behind the rim of the round window within the cochlea (insertion depth ~6 mm). The implant was fixated on the bulla using fibrin glue and dental acrylic, then the bulla opening was sealed with bone wax. Stimulation was performed with optically isolated current sources (CS1, Otoconsult, Germany).

Mapping of the primary field

Trephination was performed above the auditory cortex contralateral to the implanted ear and the dura was carefully removed using a sharp hook and ophthalmological scissors. The cortex was photographed to document the recording positions. Using an x-y-z micromotor (1 µm precision in all directions), a silver-ball macroelectrode (diameter 1 mm) was positioned at 9 cortical positions on the primary auditory cortex (field A1). The dorsal end of the posterior ectosylvian sulcus was used as a reference point. LFP signals recorded in response to a single electric biphasic pulse applied to a CI were preamplified (60 dB, Otoconsult V2 low-impedance amplifier), amplified at a second stage (20 dB, Otoconsult Amplifier-Filter F1, filters 0.010–10 kHz), recorded using National Instruments multifunctional data acquisition card (NI PCIe 6259, National Instruments, USA), and averaged (100 sweeps, repetition rate 1.97 Hz).

To determine the exact extent of the cortical activated region, a Ringer-filled glass microelectrode (impedance <6 MΩ) was used. Local field potentials (LFP) on the cortical surface were recorded at 75–150 cortical positions during stimulation with the CI, using single biphasic pulses (200 µs/phase, wide bipolar stimulation at the contralateral ear, stimulation current 10 dB above the E-ABR-threshold). Fifty responses were averaged to obtain evoked surface LFPs. Amplitudes of these middle-latency responses (peak to baseline) were used to construct cortical activation maps (Kral *et al.*, 2009) using custom-made software programmed in MATLAB© (MathWorks, Inc.).

Animal's status and condition during the experiment

End-tidal CO_2 was monitored and maintained at around 4%, and core temperature was kept above 37.5 °C using a homeothermic blanket. The animal's status was further monitored by analysis of the capillary blood aimed at gas concentration, pH, bicarbonate concentration and base excess, glycemia, ion concentration and oxygen saturation determined using IRMA TruPoint Blood Analysis System, ITC, USA. A modified Ringer's solution containing bicarbonate and plasma expander was infused i.v. with additional bicarbonate depending on the acid–base status. Monitoring and correction of the acid–base balance was performed every 12 hours.

Hearing status and deafening procedure

The speaker membrane was positioned approximately 1 cm from the tympanic membrane within a custom-made acoustically calibrated sound-delivery device (closed system) inserted into the remaining part of the external auditory meatus after the pinna was removed. Brainstem evoked signals were recorded using an epidural vertex electrode against a reference (subcutaneous silver wire) at the midline of the neck. ABR signal were preamplified (60 dB, Otoconsult V2 low-impedance amplifier), amplified at a second stage (40 dB, Otoconsult Amplifier-Filter F1, filters 0.010–10 kHz), recorded using National Instruments multifunctional data acquisition card (NI PCIe 6259, National Instruments, USA), and averaged (200 sweeps, repetition rate 33 Hz, Audiology Laboratory, Otoconsult, Frankfurt am Main, Germany). The absence of acoustically evoked brainstem responses (including wave I, generated within the auditory nerve) to clicks up to 120 dB SPL verified complete deafness. In hearing groups, the lowest thresholds had to be <40 dB SPL. Subsequently, the animals were deafened by slow instillation of 300 µL of neomycin sulfate through the round window into the scala tympani (within 5 min). The neomycin was left in place for further 5 min and later washed out by slow instillation of Ringer's solution. The total absence of brainstem evoked responses verified that the deafening procedure was successful.

References

Behrendt M. Entwicklung und Herstellung eines Cochlea-Implantates zur chronischen Stimulation von gehörlosen weißen Katzen. 1999

Kral A, Tillein J, Hubka P, Schiemann D, Heid S, Hartmann R, et al. Spatiotemporal patterns of cortical activity with bilateral cochlear implants in congenital deafness. J. Neurosci. 2009; 29: 811–27.